

Published in final edited form as:

Exp Neurol. 2012 August ; 236(2): 283–297. doi:10.1016/j.expneurol.2012.05.012.

Identification of radial glia-like cells in the adult mouse olfactory bulb

JASON G. EMSLEY^{1,2,6,*}, JOAO R.L. MENEZES^{1,2,3,*}, RODRIGO F. MADEIRO DA COSTA⁴, ANA MARIA BLANCO MARTINEZ⁵, and JEFFREY D. MACKLIS^{1,2}

¹Department of Stem Cell and Regenerative Biology, and Harvard Stem Cell Institute, Harvard University, Cambridge, MA, USA

²Department of Neurology and Program in Neuroscience, Harvard Medical School, Boston, MA, USA

³Programa de Anatomia, Instituto de Ciências Biomédicas, CCS Universidade Federal do Rio de Janeiro, Brazil

⁴Instituto de Bioquímica Médica and Programa de Pós-graduação em Química Biológica, Universidade Federal do Rio de Janeiro, Brazil

⁵Instituto de Ciências Biomédicas, Universidade Federal do Rio de Janeiro, Brazil

Abstract

Immature neurons migrate tangentially within the rostral migratory stream (RMS) to the adult olfactory bulb (OB), then radially to their final positions as granule and periglomerular neurons; the controls over this transition are not well understood. Using adult transgenic mice with the human GFAP promoter driving expression of enhanced GFP, we identified a population of radial glia-like cells that we term adult olfactory radial glia-like cells (AORGs). AORGs have large, round somas and simple, radially oriented processes. Confocal reconstructions indicate that AORGs variably express typical radial glial markers, only rarely express mouse GFAP, and do not express astroglial, oligodendroglial, neuronal, or tanycyte markers. Electron microscopy provides further supporting evidence that AORGs are not immature neurons. Developmental analyses indicate that AORGs are present as early as P1, and are generated through adulthood. Tracing studies show that AORGs are not born in the SVZa, suggesting that they are born either in the RMS or the OB. Migrating immature neurons from the adult SVZa are closely apposed to AORGs during radial migration *in vivo* and *in vitro*. Taken together, these data indicate a newly-identified population of radial glia-like cells in the adult OB that might function uniquely in neuronal radial migration during adult OB neurogenesis.

© 2012 Elsevier Inc. All rights reserved.

Address for Correspondence: Jeffrey D. Macklis, Harvard University, Department of Stem Cell and Regenerative Biology, Bauer Laboratory 103, 7 Divinity Avenue, Cambridge, MA, USA 02138, Tel: 617-495-5413, Fax: 617-496-9679, jeffrey_macklis@harvard.edu.

⁶Current address: Department of Emergency Medicine, Faculty of Medicine, Dalhousie University, Halifax, Canada

*Co-first authors

STATEMENT OF INTEREST

None.

Publisher's Disclaimer: This is a PDF file of an unedited manuscript that has been accepted for publication. As a service to our customers we are providing this early version of the manuscript. The manuscript will undergo copyediting, typesetting, and review of the resulting proof before it is published in its final citable form. Please note that during the production process errors may be discovered which could affect the content, and all legal disclaimers that apply to the journal pertain.

Keywords

astroglia; hGFAP; neurogenesis; adult olfactory radial glia-like cells (AORGs); rostral migratory stream

INTRODUCTION

Immature neurons from the anterior subventricular zone (SVZa) undergo tangential chain migration in the rostral migratory stream (RMS) into the olfactory bulb (OB), where they then migrate radially and mature into OB interneurons such as granule and periglomerular neurons (Luskin, 1993; Lois and Alvarez-Buylla, 1993, 1994; Lois *et al.*, 1996; Wichterle *et al.*, 1997; Luskin, 1998), including the periglomerular glutamatergic short axon cell (Brill *et al.*, 2009). Controls over the tangential migration of immature neurons through an extremely complex and restricted extracellular matrix have been studied extensively (Gates *et al.*, 1995; Thomas *et al.*, 1996; Peretto *et al.*, 1997); these controls include the polysialylated form of the neural cell adhesion molecule PSA-NCAM (Kiss, 1998; Chazal *et al.*, 2000; Hu, 2000), integrins (Jacques *et al.*, 1998; Emsley and Hagg, 2003), ephrins (Conover *et al.*, 2000), and Slit (Hu and Rutishauser, 1996; Wu *et al.*, 1999). However, much less is known about how migrating immature neurons make the critical developmental switch from tangential to radial migration, and are guided into their final positions as either granule or periglomerular neurons. Recent studies have shown that the extracellular matrix molecule Tenascin-R (Saghatelian *et al.*, 2004), as well as Slit (Nguyen-Ba-Charvet *et al.*, 2004) and Reelin (Hack *et al.*, 2002) can influence the radial migration of adult-born neurons. Although it is likely that the degree to which a physical substrate influences cell migration is variable, any cell types and physical substrate underlying the induction and control of radial OB migration remain unknown.

Radial glia are widespread throughout the developing CNS, acting as scaffolds for migration of neurons within the developing brain (Rakic, 1972; Hartfuss *et al.*, 2001; Rakic, 2003a). More recently, radial glia have been identified as playing a proliferative, progenitor role, rather than solely a structural role, during neocortical development (Malatesta *et al.*, 2000; Noctor *et al.*, 2001; Parnavelas and Nadarajah, 2001; Noctor *et al.*, 2002; Anthony *et al.*, 2004; Ventura and Goldman, 2007; Merkle *et al.*, 2007; Kelsch *et al.*, 2008). These and other studies have led to further characterization of the heterogeneity of type and function of radial glia in the developing CNS (Malatesta *et al.*, 2003).

Many studies have described the transformation of radial glia into typical, stellate astrocytes (Schmechel and Rakic, 1979; Alvarez-Buylla *et al.*, 1987; Hajos and Gallatz, 1987; Voigt, 1989). Studies have described a critical developmental and structural role for radial glia of providing a scaffold for both radially and tangentially migrating immature neurons (Schmechel and Rakic, 1979; Alves *et al.*, 2002; Rakic, 2003b). In combination with adhesion molecules, migrational repellents, and attractants (Hatten, 1999), radial glia have been shown to have a central role in directing and positioning newborn neurons during development (Campbell and Götz, 2002; Nadarajah and Parnavelas, 2002; Rakic, 2003b).

A number of studies have characterized the intricate temporal sequence of development of the OB (Chiu and Greer 1996; Bailey *et al.*, 1999; Puche and Shipley, 2001). These studies have described the morphology of radial glia in the developing embryonic OB, specifically noting the convoluted trajectory of the radial processes from the ventricular region to the bulb's pial surface (Puche and Shipley, 2001). However, it has been thought that radial glia disappear after embryonic development (Schmechel and Rakic, 1979; Voigt, 1989; Hunter

and Hatten, 1995). Whether there exists a cell population similarly guiding radial migration during postnatal and adult OB neurogenesis has remained unknown.

By analyzing transgenic mice that express eGFP under control of a critical regulatory region of the human GFAP promoter (Nolte *et al.*, 2001), we now identify and characterize a population of radial glia-like cells in the adult OB. Building on the previous, substantial work on olfactory radial glia during development, we describe adult olfactory radial glia-like cells (AORGs). AORGs are simple, radially oriented cells with cell bodies within the granule cell layer of the adult OB, and share multiple common characteristics with radial glial cells in other CNS regions. AORGs are abundant during early postnatal development, and some remain through adulthood. We find that some AORGs are born in the adult, in the RMS/OB itself, rather than in the SVZ overlying the lateral ventricles, and comprise a small fraction of adult born cells in the OB. Because of their phenotypic similarity to radial glia of the developing neocortex, and because of their close apposition to immature/migratory neurons in the adult OB, our data suggest that AORGs might function uniquely in controlling and guiding the final radial migration of adult-born OB neurons.

OBJECTIVE

The objective of this study was to investigate the cell type identity, characteristics, and potential function of a previously unknown and newly identified population of adult olfactory radial glia-like cells (AORGs). We hypothesized that this discrete population of glia-like cells was phenotypically distinct from migrating immature neurons of the adult rostral migratory stream/olfactory bulb, but that they share structural, immunochemical, and functional characteristics of radial glia found during early neural and OB development. To achieve our objective, we employed an array of complementary anatomical, morphological, and cell biological approaches including immunocytochemical analyses and confocal three-dimensional reconstruction, developmental studies, bromodeoxyuridine birthdating analyses, ultrastructural studies using electron microscopy, and cell culture studies using videomicroscopy.

METHODS

Mouse genotyping and anesthesia

Transgenic FVB/n mice with a 2.2 kB human glial fibrillary acidic protein (hGFAP) promoter driving expression of enhanced green fluorescent protein (eGFP) were derived from homozygous founders, kindly provided by Dr. Helmut Kettenmann (Max Delbrück Center, Berlin) (Nolte *et al.*, 2001). Heterozygous and wild-type littermates were used for all experiments reported here. Heterozygosity was confirmed either by PCR for the eGFP gene (as described in Nolte *et al.*, 2001) or by fluorescent illumination of neonatal mice under a fluorescence dissecting microscope (Nikon SMZ1500). Adult mice were housed, and all procedures were performed, according to institutional and NIH guidelines. All surgical and euthanasia procedures were performed using Avertin anesthesia beyond the neonatal period, and with hypothermia for neonatal mice.

CellTracker and Dil labeling

Adult female heterozygous mice (6-8 weeks old) were anesthetized and received stereotaxic injections of CellTracker Red (CMTPX, Molecular Probes, Eugene, OR) or DiI (5,5'-dibromo-1,1'-dioctadecyl-3,3,3',3'-tetramethylindocarbocyanine perchlorate, Molecular Probes) (Lois and Alvarez-Buylla, 1994; De Marchis *et al.*, 2001). CellTracker (10mM, 6 injections of 50 nL each) was dissolved in DMSO (Sigma, St. Louis, MO) and delivered stereotaxically via a pulled glass micropipette with a 50 μ m tip diameter into the anterior subventricular zone (SVZa) (De Marchis *et al.*, 2001) at the following coordinates: RC 1.0

mm; ML -1.1 mm; DV -2.0 mm from Bregma (after Franklin and Paxinos, 1997). DiI (0.3% in DMSO, 10 injections of 50 nL each over 4 minutes) was delivered directly into the lateral ventricle at the following coordinates: RC -0.2 mm; ML -0.9 mm; DV -2.0 mm from Bregma (Franklin and Paxinos, 1997). Mice were perfused either 7 or 21 days after CellTracker or DiI injection, and processed as below for histology.

BrdU administration

For all cell proliferation and birthdating studies, the thymidine analog 5-Bromo-2'-deoxyuridine (Sigma) was administered either as a pulse label (two injections i.p., 8 hours apart, at a concentration of 100 mg/kg body weight per injection, in sterile saline) or given for a longer period of time (7 or 21 days) at low concentration in drinking water (1.5 mg/mL) (Magavi *et al.*, 2000; Chen *et al.*, 2004); approximate dose 100 mg/kg per day).

Tissue collection and histology

For tissue collection, mice were deeply anesthetized with an approved euthanizing dose of Avertin, or via extreme hypothermia (for pups P4 or younger), and were transcardially perfused with cold 0.1 M PBS/heparin (10 U/mL) followed by cold 4% paraformaldehyde (PFA) in 0.1 M PBS (pH 7.3). Brains were carefully dissected from the skull, and were postfixed in 4% PFA at room temperature for 4 hours. Portions of the brains containing the SVZa and olfactory bulbs were removed and embedded in 4% agar. Sections (coronal or sagittal) of 30 μ m thickness were cut on a Leica VT 1000S vibrating microtome, and were stored in 0.1M PBS/0.025% sodium azide.

All immunocytochemical procedures were performed on a minimum of every 12th tissue section. Sections were rinsed in 0.1 M PBS, and blocked in 0.3% bovine serum albumin (BSA)/8% serum (e.g. goat) in 0.3% PBS-Triton X-100 (PBS-T). Native eGFP signal was enhanced with either a rabbit (1:500; Molecular Probes) or chick (1:500; Millipore/Chemicon) polyclonal antibody. Primary antibodies against glia (40E-C, A2B5, BLBP, CNPase, GalC, GFAP, GLAST, glutamine synthetase, Hes5, NG2, RC2, S100 β , and vimentin), microglia (F4/80), neurons/precursors (nestin, CD24, DARPP-32, Dcx, Hu, MAP2, NeuN, PSA-NCAM, Synaptophysin, Thy1.2, TuJ1, Tyrosine hydroxylase), cell guidance molecules/receptors (ApoE, DAB-1, Reelin, Slit1, Tenascin-R, VLDLR), and Caspase-3 were employed. The complete list of primary antibodies and their concentrations is summarized in Table 1. Primary antibodies were applied overnight at 4 °C, in blocking solution, followed by a series of PBS rinses and incubation in appropriate secondary fluorescent antibodies (1:500; Alexa 488, 546, 630; Molecular Probes) in blocking solution at room temperature for 2-4 hours. In most cases, a nuclear counterstain (DAPI, 1:5,000 in 0.1 M PBS) was also used.

For colorimetric visualization of cells for light DIC microscopy, we used an alkaline phosphatase enhancement method with avidin-biotin complex (ABC-AP), and nitro blue tetrazolium chloride/5-bromo-4-chloro-3-indolyl phosphate (NBT/BCIP; Roche, Indianapolis, IN) as the chromophore. For BrdU staining, tissue sections were treated for 2 hours at room temperature in 2 M HCl prior to application of the primary antibody. For tancyte staining, phalloidin conjugated to Alexa 494 (5 U/mL; Molecular Probes) was used as an F-actin counterstain. For Fluoro-Jade B (Schmued and Hopkins, 2000) staining, we mounted 30 μ m sections on gelatin-subbed slides. Sections were dried to the slides, rinsed in 100% EtOH, 70% EtOH, ddH₂O, and then treated in 0.06% potassium permanganate for 15 minutes. Slides were rinsed in ddH₂O, then treated with 0.001% Fluoro-Jade B (from a stock diluted in 0.1% acetic acid; Histochem) for 30 minutes. Slides were rinsed in ddH₂O, dried on a slide warmer at 45 °C for 30 minutes, rinsed in xylene, and mounted in DPX (Sigma).

Electron microscopy

Mice (as described above) were perfused with 4% paraformaldehyde, 0.4% glutaraldehyde, 5 mM CaCl₂ and 1 mM sodium cacodylate buffer. Brains were removed and post-fixed in the same fixative for 4 hours at RT. 40 μm sections were obtained with a vibrating microtome (VT1000, Leica), and were processed for GFP immunocytochemistry as described above, except that a biotinylated goat anti-rabbit antibody (1:250; Vector) was used, followed by an avidin-biotin complex (ABC), and labeling was revealed with diaminobenzidine (DAB; Vector) as the chromophore. After immunostaining, sections were rinsed in 0.1 M sodium cacodylate buffer, pH 7.4 and post-fixed in 1% OsO₄ in cacodylate buffer for 1 hr at RT. Sections were rinsed in cacodylate buffer and then dehydrated through an increasing series of ethanol to 100%, embedded in EPON between liquid-release agent-coated glass slides and coverslips at 60° C for 72 hours. After polymerization, sections were stripped from the glass slides and the region of interest in each slice was cut off and mounted on top of a resin block. Ultrathin sections (70 nm) were obtained from the mounted blocks, collected on 300 mesh copper grids and stained with 1% uranyl acetate and lead citrate. Samples were observed and imaged using a Zeiss 900 transmission electron microscope at 80 kV.

Cell culture

For primary cell culture, P1, P7, and P14 mice were deeply anesthetized, either with ice (P1) or with Avertin, as described above. Brains were carefully dissected, and the olfactory bulbs were isolated into cold dissociation medium (20 mM glucose, 0.8 mM kynurenic acid, 0.05 mM APV, 50 U/ml penicillin-0.05 mg/ml streptomycin, 0.09 M Na₂SO₄, 0.03 M K₂SO₄, and 0.014 M MgCl₂). Tissue was enzymatically digested in dissociation medium containing 0.16 g/L L-cysteine HCl and 10 U/ml papain at 37° C for 60 min. Papain digestion was blocked with dissociation medium containing 10 mg/ml ovomucoid (Sigma) and 10 mg/ml bovine serum albumin (BSA) at room temperature. Tissue was gently triturated with a flamed glass pipette in OptiMem (Invitrogen/Gibco) containing 20 mM glucose, 0.4 mM kynurenic acid, and 0.025 mM APV to protect against glutamate-induced neurotoxicity. Suspended cells were plated on poly-L-lysine (0.1 mg/mL; Sigma) coated coverslips in glial cell conditioned medium. For immunocytochemistry, cells were lightly fixed with 4% filtered PFA for 20 minutes, and immunocytochemical procedures as described above were performed with primary antibodies at the concentrations listed in Table 1. Appropriate secondary antibodies were used at a concentration of 1:500.

Videomicroscopy

For videomicroscopy of cell cultures, cover slips (with adherent cells, 30 minutes to one hour after plating) were placed in Petri dishes, with ultrathin (0.17 mm) glass bottoms (Warner Instruments). Cultures were maintained in a closed, heated chamber, supplied with warmed, humidified 5% CO₂/room air (Zeiss), mounted on a Zeiss Axiovert 200 microscope equipped with Hoffman optics and an X-Cite 120 fluorescence illuminator unit (EXFO). Images (at 40X magnification with a 1.6X optical zoom) were taken every one to three minutes with a cooled CCD camera (Photometrics Coolsnap, Roper Scientific), and collected with MetaVue image analysis software (Version 6.0). Image stacks were assembled using NIH Image J software (Version 1.31), and time-lapse movies were compiled using Quicktime Player (Version 6.5.2).

Data and image analysis

Tissue sections and cells were viewed on a Nikon E1000 microscope equipped with an X-Cite 120 fluorescence illuminator unit (EXFO). Images were acquired with a Retiga EX cooled CCD camera (QImaging), and analyzed with OpenLab image analysis software

(Version 3.5). Confocal images were acquired with a BioRad Radiance Rainbow laser scanning confocal microscope equipped for spectral imaging and mounted on a Nikon E800 microscope. Three-dimensional image reconstructions were analyzed using BioRad LaserSharp 2000 (Version 5.1), LaserVox 3-D (Version 1.0), and Imaris 4.1.3 (Bitplane) rendering software. Unless indicated otherwise, all micrographs were produced from z-stacks. All cell counts and measurements were made using NIH ImageJ software.

Cell counts were performed in a blinded fashion, with the counter unaware of the experimental condition being assessed (6 mice per assessment). Cells were only counted or measured if a full nucleus was present in the section (e.g. for nuclear labels such as NeuN), or if the cell body and its process could be visualized in the same section (e.g. for AORGs and cells positive for TuJ1 or Doublecortin (Dcx)). For total cell counts, the granule cell layer counting region was defined as the region from external to (and not including) the RMS to the external portion of the granule cell layer (defined by the internal margin of the mitral cell layer). For cell density calculations, this same region (again, excluding the RMS) was systematically divided into three concentric regions (the most central of which did not include the RMS). Measurements of cell diameters were made in an orientation perpendicular to the direction of the major process. All statistical analyses were performed with InStat software (Version 3.0a, Graphpad), and parametric (t) and non-parametric (Mann-Whitney U) tests were employed where appropriate, with a minimum significance level set at $p < 0.01$.

RESULTS

Olfactory radial glia-like cells are rare in the adult olfactory bulb

We used the broad expression of eGFP driven by the hGFAP promoter to survey the extremely varied morphologies of GFAP-positive cells throughout the developing and adult CNS. A wide variety of glial cell morphologies have been visualized in hGFAP-eGFP mice (Nolte *et al.*, 2001, Emsley and Macklis, 2006). In addition, in the adult CNS, cells with radial glia-like morphology are found at the base of the lateral ventricle (Sundholm-Peters *et al.*, 2004) as well as in the dentate gyrus, the neurogenic region of the hippocampus (Seri *et al.*, 2001; Hüttmann *et al.*, 2003). However, radial cells of the type we identify, with the distinct radial morphology of radial glia, have not been previously reported in the adult OB, using either hGFAP-eGFP mice or other methods.

The cell bodies of adult olfactory radial glia-like cells (AORGs) lie outside the outer border of the rostral migratory stream (RMS)/subventricular zone (SVZ) of the OB (in the granule cell layer), and their processes extend radially through the granule cell layer toward and into the mitral cell layer of the OB (Figs. 1A and 1A'). AORGs are morphologically very similar to those seen during embryonic and early postnatal neocortical development (Chiu and Greer 1996; Bailey *et al.*, 1999; Puche and Shipley, 2001). They have large circular somata, and long, usually straight processes (Figs. 1B and 1C) that do not bear any spines or branches. During embryonic olfactory bulb development, radial glia have an attachment to the ventricular surface, and in later stages of development such cells lose their physical connection to the ventricular zone (Puche and Shipley, 2001). Confocal reconstructions and camera lucida drawings indicate that, in contrast, AORGs do not have endfeet associated with the proliferative zone, but, rather, have short, simple, proximal processes that are not anchored to the ventricular zone (Figs. 1B and 1C). The size of AORGs is quite uniform, with typical soma diameter of approximately 7 μm and radial processes approximately 0.5 μm in diameter; these radial processes are at minimum 100 μm long, but commonly extend up to 300 μm . However, no processes extend beyond the external plexiform layer. We considered the possibility that visualization of these cells by enhancing GFP with an antibody against GFP followed by immunofluorescence might not show their complete,

detailed morphology. Therefore, we also stained selected sections with an alkaline phosphatase-based colorimetric method (with NBT/BCIP), and found the same cell morphology as observed with eGFP immunofluorescence (data not shown).

AORGs are present throughout the granule cell layer of the adult OB, with higher density closer to the RMS, and lower density closer to the mitral cell layer. To assess their relative abundance, we counted: 1) mature NeuN-positive granule cell neurons (one of the most abundant cell types in the OB); 2) doublecortin (Dcx)-positive immature migrating neurons; and 3) AORGs in the granule cell layer of the OB (excluding the RMS; per Methods). Mature NeuN-positive neurons were the most abundant (75.1%; 1,306 of 1,739 cells counted from a total of 10 sampling regions in serial sections of the olfactory bulb), followed by immature Dcx-positive neurons (22.8%; 396 of 1,739 cells counted), and AORGs (2.1%; 37 of 1,739 cells counted) (Fig. 1D).

The density of AORGs is quite low, and decreases further radially from the central portions of the OB. From three concentric regions of the granule cell layer (as described in the Methods section) we found that, while AORGs constitute approximately 10-12% of cells of the most central portion of the granule cell layer (external to and excluding the RMS), they constitute only approximately 4-5% of cells of the mid-granule cell layer, and only approximately 2-3% of cells of the outer granule cell layer. The overall density of AORGs is considerably lower than that of radial glia in the developing mammalian neocortex (Gadisseux *et al.*, 1992).

AORGs in the adult olfactory bulb are morphologically and immunochemically similar to radial glia present during early postnatal neocortical development

AORGs in the adult OB are morphologically similar to those seen with eGFP in the developing P1 neocortex; in particular, both cell populations possess slightly oblong somata with thin, outwardly directed radial processes. The size of these two morphologically similar populations of radial glia is very similar; the average soma diameter of AORGs is 7.4 ± 0.2 μm ($n=50$), which does not significantly differ from that for radial glia in the developing P1 forebrain (8.2 ± 0.3 μm ; $n=50$) ($p > 0.03$) (Fig. 2A).

As neural development progresses, there is marked heterogeneity of expression of radial glial markers throughout development (Hartfuss *et al.*, 2001). We also find considerable heterogeneity among AORGs, analogous to that seen in forebrain radial glia. Of interest is the fact that some cells that appear morphologically indistinguishable can either simultaneously express eGFP and brain-lipid binding protein (BLBP) (Feng *et al.*, 1994) (Figs 2B, B' and B'') or else express only BLBP or eGFP (Figs 2C and D). However, the occurrence of BLBP-positive cells in the adult OB is very rare, and thus the percentage of AORGs expressing BLBP is extremely low (less than approximately 5%). There are also some BLBP-positive cells in the olfactory bulb that are morphologically dissimilar to radial glia (Fig. 2D). In contrast, AORGs do not express the intermediate filament protein vimentin (Dahl *et al.*, 1981; Bailey *et al.*, 1999) (Fig. 2E), phosphorylated vimentin, nor other radial glial markers such as the glutamate transporter GLAST (Shibata *et al.*, 1997) (Fig. 2F), 40E-C (expressed by radial glia that have transformed into astroglia) (Alvarez-Buylla *et al.*, 1987) (Fig. 2G), Hes5 (Wu *et al.*, 2003) (Fig. 2H), or glutamine synthetase (data not shown). Together, these morphological and immunochemical results, along with the heterogeneity of expression of BLBP, identify AORGs as similar to, but distinct from, other forebrain radial glia.

AORGs are not neurons

We investigated the theoretical possibility that AORGs are atypical OB neurons or newly-generated immature neurons that retain hGFAP-driven expression of eGFP following generation in the SVZ. Immature neurons (“Type A cells”; Doetsch *et al.*, 1997) are present in the RMS, arising from intermediate “Type C” progenitor cells; these cells are thought to be produced by GFAP-positive progenitors (“Type B cells”) in the SVZa (Doetsch *et al.*, 1999; Doetsch, 2003). We identified many eGFP-positive immature neurons, both within the RMS and in the granule cell layer, and found that they typically co-express immature neuronal markers such as beta-III tubulin (TuJ1) (Lee *et al.*, 1990; Menezes and Luskin, 1994; Memberg and Hall, 1995) or doublecortin (Dcx) (Francis *et al.*, 1999; Gleeson *et al.*, 1999) (Fig. 3B). In addition, there are many Dcx- or TuJ1-positive immature neurons in the OB that are not eGFP-positive.

However, AORGs (identified by morphology and OB position) do not express markers of progressive neuronal differentiation. They do not express the immature neuronal markers TuJ1, Dcx (Figs. 3A-A”, 3B and 3C), PSA-NCAM, or CD24, a marker of developing neurons (Calaora *et al.*, 1996; Shewan *et al.*, 1996) (supplemental figure, D). AORGs do not exhibit mature neuronal morphology, nor do they express the early post-mitotic neuronal marker Hu (Marusich *et al.*, 1994; Barami *et al.*, 1995) (Fig. 3D), or the mature neuronal markers NeuN (Fig. 3E), MAP-2 (Fig. 3F), or Thy 1.2 (data not shown). AORGs do not express the periglomerular neuron marker tyrosine hydroxylase (supplemental figure, E). To further investigate whether AORGs receive synaptic input, we employed immunocytochemical analysis with the presynaptic marker synaptophysin (expressed at many, but not all, presynaptic terminals in the olfactory bulb), and found that AORGs do not appear to receive synaptic innervation as assessed by synaptophysin labeling (Fig. 3G).

AORGs are quite morphologically distinct from immature granule or periglomerular neurons. They are significantly larger than immature neurons, both with respect to cell body diameter and cross-sectional area. The average diameter of AORGs is $7.4 \pm 0.2 \mu\text{m}$ (SEM, $n=50$), which is significantly larger than the average diameter of TuJ1-positive neurons in the olfactory bulb ($4.9 \pm 0.2 \mu\text{m}$, SEM, $n=50$) ($p < 0.0001$, Mann-Whitney U-Test) (Fig. 3H). Similarly, the cross-sectional area of AORGs and immature neurons differs significantly; the average cross-sectional area of AORGs is $150 \pm 6.6 \mu\text{m}^2$ (SEM, $n=50$) versus $51 \pm 2.8 \mu\text{m}^2$ in TuJ1-positive immature neurons (SEM, $n=50$) ($p < 0.0001$) (Fig. 3I). In addition, AORGs are clearly not present in the periglomerular region, nor do they extend a pial process beyond the MCL, as is common for granule cells. The only eGFP-positive cells present in the periglomerular layer are stellate astroglia.

To investigate even more deeply whether AORGs might be immature neurons, we performed detailed transmission electron microscopy (EM) analysis. GFP-positive cells are rare, and readily distinguished by the presence of electron-dense DAB immunoreaction product (Fig. 4). Reaction product precipitate is present within both the cytoplasm and nucleus in a homogeneous fashion, with occasional patches (Fig. 4 B’). Because of the electron-dense reaction product and the detergent treatment necessary for revealing GFP expression, many cytoplasmic ultrastructural features, such as microtubules or intermediate filaments, are masked. However, despite this technical limitation, preserved features such as chromatin organization, cytoplasm/nucleus ratio, and unlabeled organelles including mitochondria and dense bodies (lysosomes) can be observed. We performed detailed EM analyses of a total of 8 heavily labeled cells within the granule cell layer (i.e., those considered AORGs by morphological assessment at the light microscopy level). At the ultrastructural level, AORGs are non-neuronal: they possess pale nuclei, with smooth or slightly irregular contours and poor chromatin organization (Figs. 4B and 4C). These features are compatible with immature glioblast/astrocyte phenotypes (Peretto *et al.*, 2005;

Choi, 1988; Privat, 1975; Hinds and Ruffett, 1971), and also with the relatively undifferentiated type C progenitors of the adult SVZ (Doetsch *et al.*, 1997). AORGs are generally interposed between mature granule cells, which can be easily distinguished by their large pale cytoplasm rich with organelles and rounded nuclei (Reyher *et al.*, 1991; Figs. 4B and 4C). Two other DAB-labeled cell types could also be observed by EM. The first are lightly DAB-labeled, small cells within or adjacent to the SVZ of the olfactory bulb, which were identified as neuroblasts (Fig. 4D). These cells usually included an invaginated nucleus, with slightly darker cytoplasm and nucleus (Lois *et al.*, 1996). The second cell type was found in the periglomerular, or external plexiform layer, and was always heavily labeled by the DAB immunoreaction product (Fig. 4E). These cells have the EM characteristics of fibrous astrocytes, including their typical irregularly shaped nuclei with highly organized chromatin (Peters *et al.*, 1991). Further, no DAB-positive oligodendrocytes or microglia were found in any of the specimens analyzed with EM.

AORGs rarely express astroglial markers

We investigated whether AORGs, identified by their expression of eGFP driven by the hGFAP promoter, also express GFAP protein. We found that eGFP-positive AORGs do not express GFAP, assessed by immunocytochemistry and confocal microscopic reconstructions (Fig. 5A). In agreement with a prior report (Nolte *et al.*, 2001), we find that eGFP-positive cells in other brain regions only very rarely express GFAP, and this rare co-expression of GFAP is typically limited to fine processes of GFAP-positive astroglia. AORGs only rarely express the alternate astroglial marker S100 β (Ludwin *et al.*, 1976), but never display expression of A2B5 (Raff *et al.*, 1983) (Figs. 5B and 5C).

AORGs are not oligodendroglia

We also investigated whether AORGs are members of the oligodendroglial lineage. AORGs do not co-express the proteoglycan NG2 (Stallcup and Beasley, 1987) (Fig. 5D), CNPase (2', 3'-cyclic nucleotide 3'-phosphodiesterase) (McMorris *et al.*, 1984) (Fig. 5E), or the mature oligodendroglial marker galactosylcerebroside (GalC) (Ranscht *et al.*, 1982) (Fig. 5F).

AORGs are not tanycytes, microglia, or olfactory ensheathing cells, nor are they nestin-positive

We investigated the unlikely possibility that AORGs are tanycytes, a form of elongated epithelial cell commonly found lining the CNS ventricles (Goslar and Bock, 1971). AORGs are not tanycytes by either location or immunochemical analysis for tanycyte markers. AORGs are not labeled with the F-actin stain phalloidin (Phalloidin-594), nor do they express the dopamine- and cAMP-regulated phosphoprotein DARPP-32 (data not shown). DARPP-32, though more commonly used as a marker for medium spiny neurons of the striatum (Ouimet and Greengard, 1990) is also a label for tanycytes (Hokfelt *et al.*, 1988).

Similarly, AORGs are not microglia, olfactory ensheathing cells, or nestin-positive progenitors. AORGs do not express the microglial marker F4/80 (Leenen *et al.*, 1994) (supplemental figure, B). AORGs do not express the olfactory ensheathing cell markers GFAP or O4 (Au and Roskams, 2003) (supplemental figure, C). AORGs do not express the intermediate filament protein nestin, often expressed by early neural progenitor cells (Lendahl *et al.*, 1990) (supplemental figure, A).

Taken together, these morphological and immunochemical characterizations indicate that AORGs are a new form of adult forebrain radial glia-like cells, and are not neurons, astroglia, oligodendroglia, microglia, or tanycytes. The presence of adult radial glia-like cells in the OB, the site of ongoing adult neurogenesis and radial migration from the RMS

into the OB itself, suggests that AORGs might function critically in the radial migration of adult-born neurons.

Lack of association of cell guidance molecules with AORGs

Several molecules, including Tenascin-R (Saghatelyan *et al.*, 2004), Slit1 (Wu *et al.*, 1999; Nguyen-Ba-Charvet *et al.*, 2004), and Reelin (D'Arcangelo *et al.*, 1997; Hack *et al.*, 2002) play critical roles in the migration and guidance of newly-generated immature neurons. While it is not possible using immunocytochemistry to detect whether AORGs secrete any of these cell guidance molecules (data not shown), we found that AORGs do not express the Reelin receptors ApoER2 or VLDLR, or the Reelin adaptor protein Disabled-1 (Dab-1; data not shown) (Hiesberger *et al.*, 1999; Trommsdorff *et al.*, 1999; Rice and Curran, 2001).

AORGs are born during development and in the adult

AORGs are present as early as P1, and are much more abundant at P1 than at P7, P14, or adulthood. AORGs at P1, P7, P14, and adulthood are morphologically indistinguishable. AORGs are also morphologically indistinguishable from radial glia in the developing neocortex.

We investigated when AORGs present in the adult OB are born, using postnatal injections of BrdU and examination in 8 week old adults. Examination of the adult OB following injection of BrdU at P14 indicates that AORGs are born as early as P14 (data not shown). BrdU injections at an earlier developmental time (P2) did not yield labeled adult AORGs. This result suggests that BrdU might have been diluted following multiple cell divisions from earlier precursor proliferation. Interestingly, administration of BrdU to adult mice demonstrates that AORGs continue to be born in the adult OB (Fig. 6A). Taken together, these data suggest both developmental and limited adult birth of AORGs that are present in adulthood.

Adult-born AORGs comprise approximately 3% of all of the adult-born cells throughout the entire granule cell layer of the adult OB (141 of 4,177 BrdU-positive cells counted by random sampling of multiple sections of the adult OB). In contrast, our data and that of others reveals that approximately 95% of BrdU-positive adult-born cells differentiate into mature, NeuN-positive neurons (Winner *et al.*, 2002; Magavi *et al.*, 2005). There are no substantial differences in the number of adult-born AORGs in different regions of the adult OB along its rostral to caudal extent, suggesting that AORG generation and incorporation is relatively uniform in the adult OB, and that there are no proliferation “hot spots” for production of AORGs in the adult OB.

Adult born AORGs become mature in 10-14 days and exhibit long-term survival in the OB

We investigated the time course of development of AORGs in the adult OB, from 3 to 35 days after administration of a single pulse label of BrdU. Consistent with previously reported data, we found that, 3 days after BrdU administration, BrdU-positive/eGFP-negative cells are present throughout the RMS and granule cell layer of the OB (Menezes *et al.*, 1995; Winner *et al.*, 2002; Magavi *et al.*, 2005). Newborn, BrdU-positive/eGFP-positive cells are found only in proximity to the RMS after three days; at three days, no mature AORGs are BrdU-positive, and no BrdU-positive cells are yet AORGs. The very few BrdU-positive/eGFP-positive cells present at day 3 possess round somas with short radial processes (Fig. 6B). By 7 days, BrdU-positive/eGFP-positive cells with somewhat elongated processes exist (Fig. 6C), occasionally within the granule cell layer. By days 10 and 14, BrdU-positive/eGFP-positive AORGs possess mature morphology (Fig. 6D). Consistent with prior reports (Petreanu and Alvarez-Buylla, 2002; Winner *et al.*, 2002; Magavi *et al.*, 2005), 14 days after their birth, many large BrdU-positive/eGFP-negative adult-born

interneurons reside in the granule cell layer. Adult-born, BrdU-positive AORGs maintain their eGFP-positive morphology and long radially oriented processes 21 and 35 days after their birth. This mature AORG morphology is quite distinct from that already exhibited by adult-born granule neurons by 21-35 days (Kishi, 1987; Petreanu and Alvarez-Buylla, 2002); granule neurons have complex arborization even by day 21, in addition to their significantly different soma size.

We investigated the theoretical possibility that AORGs might be largely a transient population, with only a smaller population surviving in the adult. However, experiments did not detect substantial amounts of cell death. Specifically, AORGs are not labeled with the cell death markers cleaved caspase-3 (Kuida *et al.*, 1996) or Fluoro-Jade B (Schmued and Hopkins, 2000); adult mice were administered BrdU and analyzed 3 and 6 weeks later for cell death markers. There was an average of 1.4 ± 0.2 eGFP-positive/BrdU-positive AORGs per section in the 3 week survival group versus 1.2 ± 0.3 eGFP-positive/BrdU-positive AORGs per section in the 6 week survival group, and this difference was not significant ($p < 0.5873$). These results indicate that there is very little ongoing death of AORGs in the adult OB, and support the interpretation that AORGs are not a transient population, but, rather, are a long-lived population in the adult. These results also suggest the possibilities that AORGs might be differentiating into astrocytes, losing eGFP expression, or even returning to the cell cycle.

AORGs are born locally in the olfactory bulb

We investigated whether AORGs are generated in the anterior SVZ (SVZa), a region known to produce immature neurons that migrate via the RMS to the OB (Lois and Alvarez-Buylla, 1994). We injected CellTracker Red into the SVZa (De Marchis *et al.*, 2001) or DiI into the lateral ventricle (Lois and Alvarez-Buylla, 1994). Seven and 21 days after injection, many dye-labeled cells were present in the RMS, but very few of these were also eGFP-positive. 21 days after CellTracker Red or DiI injection, there were fully mature, dye-labeled granule cells in the OB (Figs. 6G and 6H), and of the 594 CellTracker Red cells analyzed, none was a dye-labeled AORG. Intriguingly, many of the dye-labeled migrating immature neurons are positioned in close apposition to the long radial processes of AORGs (Figs. 6F, 6G, and 6H), suggesting a possible interaction during radial migration of neurons. Taken together, these data indicate that AORGs are born either in the RMS or in the parenchyma of the OB, rather than in the SVZa (where most adult-born neurons originate), and suggest a physical interaction of AORGs with newborn immature neurons migrating radially in the adult OB.

Immature OB neurons are found close to AORG radial processes in vitro

AORGs retain their radial morphology *in vitro*, assessed in primary dissociated cultures of P7 and P14 OB (Fig. 7). AORGs are considerably less abundant than most other cell types in the OB (neuroblasts, granule neurons, and astroglia). It appears, however, that at least some immature neurons (including those that are eGFP-positive) are found closely apposed to AORGs in these cultures, and every AORG is observed to have smaller, immature neurons in close apposition to its major process and soma (Figs. 7A and 7B). Videomicroscopy of P7 cultures reveals immature neurons apposed to the somas and radial processes of AORGs, and appear to sometimes initiate migration (Figs. 7C and 7D). Taken together with 1) the known functions of radial glia in neuronal migration in other CNS regions; 2) the data on AORG radial morphology in the adult OB; 3) their identification as related to developmental forebrain radial glia; and 4) their stability in this form in the adult OB, these data showing close apposition of immature, migratory neurons *in vivo* and *in vitro* suggest that AORGs might likely function in radial migration of adult-born neurons into the body of the OB during ongoing adult neurogenesis.

CONCLUSIONS

1. We have identified a rare population of adult olfactory radial glia-like cells (AORGs), which are radially oriented in the olfactory bulb, and which share morphological and immunochemical characteristics of forebrain radial glia.
2. AORGs are morphologically, immunochemically, and ultrastructurally distinct from astroglia, oligodendroglia, tanycytes, and neurons.
3. AORGs are born in the rostral migratory stream or olfactory bulb, both developmentally and in the adult, and exhibit long-term survival.
4. Immature olfactory bulb neurons are found in close association with AORG radial processes *in vivo* and *in vitro*.

DISCUSSION

We report the identification of radial glia-like cells in the adult OB for the first time; these adult olfactory radial glia-like cells (AORGs) have several unique defining characteristics. AORGs possess large, round somas and non-arborized, exclusively radially oriented processes, directed away from the core of the RMS of the adult OB. AORGs are rare, and comprise a very small percentage of the cells found in the adult OB. AORGs possess a variety of features very similar to those of radial glial cells present during normal embryonic and early postnatal neocortical and striatal development; AORGs are neither immature neurons nor astroglia. *In vivo*, *in vitro*, and videomicroscopic analyses also suggest that immature, migratory OB neurons are often closely apposed to AORG radial processes. Taken together, our data suggest that AORGs might likely function in directing the radial migration of immature neurons during adult OB neurogenesis.

Although increasingly detailed phenotypic characterization of a variety of astroglial, oligodendroglial, neuronal, and precursor cell types in the adult CNS is the subject of much research, there have been very few reports in the past century describing a new cell type. A novel neuronal phenotype generated from hypothalamic progenitor cells *in vitro* has been reported recently (Markakis *et al.*, 2004), and radial glia-like cells in the ventral portion of the lateral ventricle, present in the embryo as well as in limited regions in the adult lateral ventricle, have also been reported recently (Sundholm-Peters *et al.*, 2004; Gubert *et al.*, 2009). The fact that other brain regions contain radial glia-like cells that do not transform into stellate astroglia is consistent with our findings that radial glia continue to exist and be produced in the adult OB. Indeed, the production and maintenance of cells with the radial glial phenotype in the SVZ and striatum of the adult CNS has been reported, both in neural stem cell cultures and *in vivo* (Gregg and Weiss, 2003), as well as in response to targeted neocortical neuron death in the adult mouse (Leavitt *et al.*, 1999), following placement of astrocytes into an embryonic environment or embryonic conditioned medium (Hunter and Hatten, 1995), or after transplantation of embryonic Cajal-Retzius cells into the adult cerebellum (Soriano *et al.*, 1997). In addition, the existence of radial glia-like cells in the other well-characterized neurogenic region of the adult brain, the dentate gyrus of the hippocampal formation (Seri *et al.*, 2001; Hüttmann *et al.*, 2003; Shapiro *et al.*, 2005), presents an opportunity to explore as yet undefined shared markers or molecular signatures in common between AORGs and the radial glia of the adult dentate gyrus.

The hGFAP-eGFP promoter enables initial identification of AORGs

We originally used transgenic mice with the human GFAP (hGFAP) promoter driving eGFP expression (Nolte *et al.*, 2001) in order to visualize stellate astroglia in the adult CNS. However, the GFAP gene itself is highly regulated, and numerous transcriptional

mechanisms control the subsequent translation of GFAP protein. Indeed, there can be great variability in GFAP transgene expression; such variability is related to the specific promoter used, and to the type of reporter being employed (such as *LacZ* or GFP). In the mouse line we used, a segment of approximately 2.2kb upstream of the human GFAP gene is sufficient to drive gene expression in astroglial cells in the brain (Brenner *et al.*, 1994; Zhuo *et al.*, 1997; Nolte *et al.*, 2001; Su *et al.*, 2004), as is the equivalent segment in the mouse (Johnson *et al.*, 1995). The imperfect overlap of eGFP reporter and GFAP protein expression has been described previously for this particular transgenic mouse line (Nolte *et al.*, 2001) and in other similar transgenic models (Brenner *et al.*, 1994; Su *et al.*, 2004). This imperfect match between expression of the transgene and GFAP protein is likely due to higher sensitivity of the reporter protein, a lack of other regulatory sequences, and low endogenous expression of GFAP protein by some astrocytes, such as gray matter astrocytes (Ludwin *et al.*, 1976; Kalman and Hajos, 1989). However, consistent with the glial nature of the hGFAP promoter activity, we did not detect ectopic expression of the reporter outside of the nervous system (data not shown). Regardless of the inconsistency between GFAP protein expression and hGFAP driven expression of eGFP, the robust expression of eGFP provided an opportunity to detect cells of a unique, radial glia-like morphology.

The presence of GFAP, while often taken as evidence that expressing cells are astroglial, does not necessarily mean that a cell is a true astrocyte. Indeed, some forebrain precursor cells might also express GFAP (Doetsch *et al.*, 1999). We found hGFAP-eGFP-positive cells in the RMS and the OB that are Dcx-positive and are labeled by CellTracker Red injected into the SVZa, indicating that these cells are likely the progeny of GFAP-positive precursors in the SVZ. Thus, GFAP, while generally a reliable marker for activated astroglia, cannot be used as a sole phenotypic marker of astroglia. In addition, it is widely understood that GFAP immunocytochemistry does not provide an accurate indication of the number of astroglia.

In contrast to the homologous GFAP promoter region in mice (Galou *et al.*, 1994), the human GFAP promoter drives gene expression in multipotential progenitors during early development (Brenner *et al.*, 1994; Malatesta *et al.*, 2000, 2003), well before GFAP expression is detectable in mice (Galou *et al.*, 1994). Detailed analysis of eGFP expression driven by this hGFAP promoter in adult transgenic mice suggests that there is considerable cellular, and specifically astroglial, heterogeneity in the adult CNS (Emsley and Macklis, 2006). These latter results are consistent with earlier descriptions of astroglial heterogeneity in the CNS (Prochiantz and Mallat, 1988; Scotti Campos, 2003).

AORGs are very similar to radial glia seen during CNS development

We present several independent lines of evidence that AORGs are radial glia-like cells rather than neurons, oligodendroglia, typical astroglia, or other cell types. hGFAP promoter expression of eGFP cannot serve as a sole phenotypic indicator, due to the specifics of GFAP expression and processing discussed above. The identification of AORGs as a novel population of radial glia-like cells is based on a combination of morphology and both positive and exclusionary phenotypic protein expression. Light, fluorescence, and electron microscopy studies indicate that AORGs are very similar in size, shape, and ultrastructural characteristics to “classical” radial glia present during neocortical development. Further, AORGs rarely express classical astroglial markers, but largely express classical radial glial markers, such as brain lipid binding protein (BLBP). Interestingly, AORGs do not express vimentin, known to be expressed by radial glia of the developing OB (Bailey *et al.* 1999).

AORGs are born locally

Two lines of evidence suggest that AORGs are produced locally in the RMS or parenchyma of the OB, rather than in the SVZ. The first set of data supporting this conclusion comes

from experiments in which CellTracker Red or DiI were used to label cells originating in the SVZ. Although immature neurons that were labeled with CellTracker Red or DiI and were eGFP-positive were present in the RMS (likely the progeny of GFAP-expressing precursors), there were no CellTracker Red or DiI stained eGFP-positive AORGs in the adult OB. Importantly, there were CellTracker Red or DiI stained immature neurons closely apposed to eGFP-positive AORGs (unlabeled by CellTracker Red or DiI) in the granule cell layer 7 days after injection, and mature granule cell interneurons stained with CellTracker Red or DiI were present in the granule cell layer 21 days after SVZa dye injection.

A second line of evidence that AORGs do not originate in the SVZa derives from the cell proliferation experiments. Injection of a single pulse of BrdU, followed by analysis either 3 or 7 days later, revealed small, BrdU-positive/eGFP-positive cells lacking either mature AORG morphology or the long migratory processes of TuJ1-positive neuroblasts. This observation indicates that AORGs are born in the RMS/OB and undergo migration locally, with extension of their radial processes over 7-14 days following their birth. It will be of interest to investigate these cells' lineage, motility, and proliferative capacity in more detail.

Why were AORGs previously undetected?

After so much interest in the OB as a model of adult neurogenesis, it might seem surprising that AORGs have not been detected previously. However, there are two simple reasons: their rarity, and their lack of expression of most common cell-type phenotypic markers. Since AORGs make up only an extremely small percentage of cells in the adult OB (and only ~ 2% even in the granule cell layer, where they reside and are at maximal concentration), it is not surprising that they escaped detection. Their lack of labeling with most immunochemical markers would have made their detection extremely difficult. AORGs might likely have been grouped with other OB cell types, e.g. immature migrating neurons. However, detailed confocal microscopic analysis and reconstructions, analyses of TuJ1 and Dcx expression, electron microscopy, and morphometric measurements all reveal that AORGs are quite distinct. Importantly, the hGFAP promoter serendipitously enabled AORG identification because the rare AORGs would likely not be detected by Golgi staining (which only labels a small fraction of any cell population, and thus might be expected to label vanishingly few AORGs) or other methods. In addition, approximately 95-97% of newborn cells in the adult OB differentiate into mature neuronal phenotypes (Winner *et al.*, 2002; Magavi *et al.*, 2005), and this rare population of cells might account for at least some of the remaining ~ 3-5% of newborn cells in the adult OB.

Do AORGs act as a physical substrate for radial migration of adult-born OB neurons?

Though some of the molecular factors contributing to the transition by adult-born OB neurons from tangential to radial migration are known, the process is not well understood. These factors include Reelin (Hack *et al.*, 2002), Tenascin-R (Saghatelian *et al.*, 2004), ADAM2 (Murase *et al.*, 2008), and IGF-1 (Hurtado-Chong *et al.*, 2009). In addition, it has recently been shown that astroglial permissivity to migration differs along the RMS, thereby influencing movement of immature neurons destined for the olfactory bulb (Garcia-Marqués *et al.*, 2010). AORGs are not immunopositive for Reelin and, because Tenascin-R is an extracellular matrix molecule with diffuse expression throughout the parenchyma (Gates *et al.*, 1995; Thomas *et al.*, 1996), immunocytochemistry cannot conclusively determine whether it is secreted by AORGs. It would be of interest in the future to investigate whether AORGs express other guidance-related and/or chemo-attractant molecules.

It is interesting to speculate that adult-born AORGs might likely function in the transition of migrating, immature neurons from tangential migration through the RMS to radial migration into the OB parenchyma. Additionally, AORGs might provide a cellular substrate for such

immature neurons to reach their proper positions primarily within the granule cell layer, or they might provide directional guidance as far as the mitral cell layer for the smaller population of adult-born periglomerular neurons. It would be of interest to investigate possible cellular interactions of AORGs with adult-born OB neurons, and molecular mechanisms underlying their potential role in radial migration during adult olfactory bulb neurogenesis.

Supplementary Material

Refer to Web version on PubMed Central for supplementary material.

Acknowledgments

We thank Alex Eswar, Kyle MacQuarrie, Ashley Palmer, Karen Billmers, and Aaron Wheeler for excellent technical assistance, and other members of the Macklis laboratory for their many helpful comments. The transgenic hGFAP-eGFP mouse line was a generous gift from Drs. Helmut Kettenmann and Christiane Nolte (Max Delbrück Center for Molecular Medicine, Berlin). We thank Dr. Tatjana Jakobs (MGH, HMS) for sharing her expertise with videomicroscopy, and Dr. Richard Masland (MGH, HMS) for the use of the videomicroscopy equipment. We thank Dr. Nathaniel Heintz (Rockefeller University) for the gift of BLBP antibody; Dr. Pam Follett (Children's Hospital, Boston) for the gift of A2B5 antibody; and Dr. Ron McKay (NIH) for the gift of the nestin antibody. We thank Carol Birmingham and Chemicon/Millipore for the gift of several antibodies. Several monoclonal antibodies were obtained from the Developmental Studies Hybridoma Bank, developed under the auspices of the NICHD and maintained by The University of Iowa, Department of Biological Sciences, Iowa City. This work was supported by NIH grants NS45523 and NS49553 (to J.D.M.), with additional infrastructure provided by NS41590 (to J.D.M.); grants from the Children's Neurobiological Solutions Foundation and United Sydney Foundation (to J.D.M.); and CNPq-Brazil and an NIH-NINDS International Fellowship (to J.R.L.M.). J.G.E. was partially supported by fellowships from the Heart and Stroke Foundation of Canada, the Paralyzed Veterans of America/Travis Roy Foundation, and the Curry Endowment of the Dalhousie Medical Research Foundation.

REFERENCES

- Alvarez-Buylla A, Buskirk DR, Nottebohm F. Monoclonal antibody reveals radial glia in adult avian brain. *Journal of Comparative Neurology*. 1987; 264:159–170. [PubMed: 2445794]
- Alves JA, Barone P, Engelender S, Froes MM, Menezes JR. Initial stages of radial glia astrocytic transformation in the early postnatal anterior subventricular zone. *Journal of Neurobiology*. 2002; 52:251–265. [PubMed: 12210108]
- Anthony TE, Klein C, Fishell G, Heintz N. Radial glia serve as neuronal progenitors in all regions of the central nervous system. *Neuron*. 2004; 41:881–890. [PubMed: 15046721]
- Au E, Roskams AJ. Olfactory ensheathing cells of the lamina propria in vivo and in vitro. *Glia*. 2003; 41:224–236. [PubMed: 12528178]
- Bailey MS, Puche AC, Shipley MT. Development of the olfactory bulb, evidence for glia-neuron interactions in glomerular formation. *Journal of Comparative Neurology*. 1999; 415:423–448. [PubMed: 10570454]
- Barami K, Iversen K, Furneaux H, Goldman SA. Hu protein as an early marker of neuronal phenotypic differentiation by subependymal zone cells of the adult songbird forebrain. *Journal of Neurobiology*. 1995; 28:82–101. [PubMed: 8586967]
- Brenner M, Kisseberth WC, Su Y, Besnard F, Messing A. GFAP promoter directs astrocyte-specific expression in transgenic mice. *Journal of Neuroscience*. 1994; 14:1030–1037. [PubMed: 8120611]
- Brill MS, Ninkovic J, Winpenny E, Hodge RD, Ozen I, Yang R, Lepier A, Gascón S, Erdelyi F, Szabo G, Parras C, Guillemot F, Frotscher M, Berninger B, Hevner RF, Raineteau O, Götz M. Adult generation of glutamatergic olfactory bulb interneurons. *Nature Neuroscience*. 2009; 12:1524–1533.
- Calaora V, Chazal G, Nielsen PJ, Rougon G, Moreau H. mCD24 expression in the developing mouse brain and in zones of secondary neurogenesis in the adult. *Neuroscience*. 1996; 73:581–594. [PubMed: 8783272]
- Campbell K, Götz M. Radial glia: multi-purpose cells for vertebrate brain development. *Trends in Neurosciences*. 2002; 25:235–238. [PubMed: 11972958]

- Chazal G, Durbec P, Jankovski A, Rougon G, Cremer H. Consequences of neural cell adhesion molecule deficiency on cell migration in the rostral migratory stream of the mouse. *Journal of Neuroscience*. 2000; 20:1446–1457. [PubMed: 10662835]
- Chen J, Magavi SS, Macklis JD. Neurogenesis of corticospinal motor neurons extending spinal projections in adult mice. *Proceedings of the National Academy of Sciences*. 2004; 101:16357–16362.
- Chiu K, Greer CA. Immunocytochemical analyses of astrocyte development in the olfactory bulb. *Brain Research Developmental Brain Research*. 1996; 95:28–37. [PubMed: 8873973]
- Choi BH. Prenatal gliogenesis in the developing cerebrum of the mouse. *Glia*. 1988; 1:308–316. [PubMed: 2976394]
- Conover JC, Doetsch F, Garcia-Verdugo JM, Gale NW, Yancopoulos GD, Alvarez-Buylla A. Disruption of Eph/ephrin signaling affects migration and proliferation in the adult subventricular zone. *Nature Neuroscience*. 2000; 3:1091–1097.
- D'Arcangelo G, Nakajima K, Miyata T, Ogawa M, Mikoshiba K, Curran T. Reelin is a secreted glycoprotein recognized by the CR-50 monoclonal antibody. *Journal of Neuroscience*. 1997; 17:23–31. [PubMed: 8987733]
- Dahl D, Rueger DC, Bignami A, Weber K, Osborn M. Vimentin, the 57 000 molecular weight protein of fibroblast filaments, is the major cytoskeletal component in immature glia. *European Journal of Cell Biology*. 1981; 24:191–196. [PubMed: 7285936]
- De Marchis S, Fasolo A, Shipley M, Puche A. Unique neuronal tracers show migration and differentiation of SVZ progenitors in organotypic slices. *Journal of Neurobiology*. 2001; 49:326–338. [PubMed: 11745668]
- Doetsch F. The glial identity of neural stem cells. *Nature Neuroscience*. 2003; 6:1127–1134.
- Doetsch F, Caille I, Lim DA, Garcia-Verdugo JM, Alvarez-Buylla A. Subventricular zone astrocytes are neural stem cells in the adult mammalian brain. *Cell*. 1999; 97:703–716. [PubMed: 10380923]
- Doetsch F, Garcia-Verdugo JM, Alvarez-Buylla A. Cellular composition and three-dimensional organization of the subventricular germinal zone in the adult mammalian brain. *Journal of Neuroscience*. 1997; 17:5046–5061. [PubMed: 9185542]
- Emsley JG, Macklis JD. Astroglial heterogeneity closely reflects the neuronal-defined anatomy of the adult murine CNS. *Neuron Glia Biology*. 2006; 2:175–186. [PubMed: 17356684]
- Emsley JG, Hagg T. alpha6beta1 integrin directs migration of neuronal precursors in adult mouse forebrain. *Experimental Neurology*. 2003; 183:273–285. [PubMed: 14552869]
- Feng L, Hatten ME, Heintz N. Brain lipid-binding protein (BLBP): a novel signaling system in the developing mammalian CNS. *Neuron*. 1994; 12:895–908. [PubMed: 8161459]
- Francis F, Koulakoff A, Boucher D, Chafey P, Schaar B, Vinet MC, Friocourt G, McDonnell N, Reiner O, Kahn A, McConnell SK, Berwald-Netter Y, Denoulet P, Chelly J. Doublecortin is a developmentally regulated, microtubule-associated protein expressed in migrating and differentiating neurons. *Neuron*. 1999; 23:247–256. [PubMed: 10399932]
- Franklin, KBJ.; Paxinos, G. *The Mouse Brain in Stereotaxic Coordinates*. Academic Press; 1997.
- Gadisseux JF, Evrard P, Mission JP, Caviness VS Jr. Dynamic changes in the density of radial glial fibers of the developing murine cerebral wall: a quantitative immunohistological analysis. *Journal of Comparative Neurology*. 1992; 322:246–254. [PubMed: 1522252]
- Galou M, Pourmin S, Ensergueix D, Ridet JL, Tchelingirian JL, Lossouarn L, Privat A, Babinet C, Dupouey P. Normal and pathological expression of GFAP promoter elements in transgenic mice. *Glia*. 1994; 12:281–293. [PubMed: 7890332]
- Garcia-Marqués J, De Carlos JA, Greer CA, López-Mascaraque L. Different astroglial permissivity controls the migration of olfactory bulb interneuron precursors. *Glia*. 2010; 58:218–230. [PubMed: 19610095]
- Gates MA, Thomas LB, Howard EM, Laywell ED, Sajin B, Faissner A, Götz B, Silver J, Steindler DA. Cell and molecular analysis of the developing and adult mouse subventricular zone of the cerebral hemispheres. *Journal of Comparative Neurology*. 1995; 361:249–266. [PubMed: 8543661]
- Gleeson JG, Lin PT, Flanagan LA, Walsh CA. Doublecortin is a microtubule-associated protein and is expressed widely by migrating neurons. *Neuron*. 1999; 23:257–271. [PubMed: 10399933]

- Goslar HG, Bock R. Histochemical properties of the unspecific esterases in the tancyte ependyma of the third ventricle, in the subfornical organ and in the subcommissural organ of the wistar rat. *Histochemie*. 1971; 28:170–182. [PubMed: 5137665]
- Gregg C, Weiss S. Generation of functional radial glial cells by embryonic and adult forebrain neural stem cells. *Journal of Neuroscience*. 2003; 23:11587–11601. [PubMed: 14684861]
- Gubert F, Zaverucha-do-Valle C, Pimentel-Coelho PM, Mendez-Otero R, Santiago MF. Radial glia-like cells persist in the adult rat brain. *Brain Research*. 2009; 1258:43–52. [PubMed: 19124008]
- Hack I, Bancila M, Loulier K, Carroll P, Cremer H. Reelin is a detachment signal in tangential chain-migration during postnatal neurogenesis. *Nature Neuroscience*. 2002; 5:939–945.
- Hajos F, Gallatz K. Immunocytochemical demonstration of radial glia in the developing rat olfactory bulb with antibodies to glial fibrillary acidic protein. *Brain Research*. 1987; 433:131–138. [PubMed: 3676849]
- Hartfuss E, Galli R, Heins N, Götz M. Characterization of CNS precursor subtypes and radial glia. *Developmental Biology*. 2001; 229:15–30. [PubMed: 11133151]
- Hatten ME. Central nervous system neuronal migration. *Annual Review of Neuroscience*. 1999; 22:511–539.
- Hiesberger T, Trommsdorff M, Howell BW, Goffinet A, Mumby MC, Cooper JA, Herz J. Direct binding of Reelin to VLDL receptor and ApoE receptor 2 induces tyrosine phosphorylation of disabled-1 and modulates tau phosphorylation. *Neuron*. 1999; 24:481–9. [PubMed: 10571241]
- Hinds JW, Ruffett TL. Cell proliferation in the neural tube: an electron microscopic and golgi analysis in the mouse cerebral vesicle. *Z. Zellforsch*. 1971; 115:226–264. [PubMed: 4102323]
- Hokfelt T, Foster G, Schultzberg M, Meister B, Schalling M, Goldstein M, Hemmings HC Jr, Ouimet C, Greengard P. DARPP-32 as a marker for D-1 dopaminergic cells in the rat brain: prenatal development and presence in glial elements (tancytes) in the basal hypothalamus. *Advances in Experimental Medicine and Biology*. 1988; 235:65–82. [PubMed: 2976255]
- Hu H. Polysialic acid regulates chain formation by migrating olfactory interneuron precursors. *Journal of Neuroscience Research*. 2000; 61:480–492. [PubMed: 10956417]
- Hu H, Rutishauser U. A septum-derived chemorepulsive factor for migrating olfactory interneuron precursors. *Neuron*. 1996; 16:933–940. [PubMed: 8630251]
- Hurtado-Chong A, Yusta-Boyo MJ, Vergaño-Vera E, Bulfone A, de Pablo F, Vicario-Abejón C. IGF-1 promotes neuronal migration and positioning in the olfactory bulb and the exit of neuroblasts from the subventricular zone. *European Journal of Neuroscience*. 2009; 30:742–755. [PubMed: 19712103]
- Huttmann K, Sadgrove M, Wallraff A, Hinterkeuser S, Kirchhoff F, Steinhäuser C, Gray WP. Seizures preferentially stimulate proliferation of radial glia-like astrocytes in the adult dentate gyrus: functional and immunocytochemical analysis. *European Journal of Neuroscience*. 2003; 18:2769–2778. [PubMed: 14656326]
- Hunter KE, Hatten ME. Radial glial cell transformation to astrocytes is bidirectional: regulation by a diffusible factor in embryonic forebrain. *Proceedings of the National Academy of Sciences*. 1995; 92:2061–2065.
- Jacques TS, Relvas JB, Nishimura S, Pytela R, Edwards GM, Streuli CH, French-Constant C. Neural precursor cell chain migration and division are regulated through different beta1 integrins. *Development*. 1998; 125:3167–3177. [PubMed: 9671589]
- Johnson WB, Ruppe MD, Rockenstein EM, Price J, Sarthy VP, Verderber LC, Mucke L. Indicator expression directed by regulatory sequences of the glial fibrillary acidic protein (GFAP) gene: in vivo comparison of distinct GFAP-lacZ transgenes. *Glia*. 1995; 13:174–184. [PubMed: 7782103]
- Kalman M, Hajos F. Distribution of glial fibrillary acidic protein (GFAP)-immunoreactive astrocytes in the rat brain. I. Forebrain. *Experimental Brain Research*. 1989; 78:147–163.
- Kelsch W, Lin CW, Lois C. Sequential development of synapses in dendritic domains during adult neurogenesis. *Proceedings of the National Academy of Sciences*. 2008; 105:16803–16808.
- Kishi K. Golgi studies on the development of granule cells of the rat olfactory bulb with reference to migration in the subependymal layer. *Journal of Comparative Neurology*. 1987; 258:112–124. [PubMed: 3571532]

- Kiss JZ. A role of adhesion molecules in neuroglial plasticity. *Molecular and Cellular Endocrinology*. 1998; 140:89–94. [PubMed: 9722174]
- Kuida K, Zheng TS, Na S, Kuan C, Yang D, Karasuyama H, Rakic P, Flavell RA. Decreased apoptosis in the brain and premature lethality in CPP32-deficient mice. *Nature*. 1996; 384:368–372. [PubMed: 8934524]
- Leavitt BR, Hermit-Grant CS, Macklis JD. Mature astrocytes transform into transitional radial glia within adult mouse neocortex that supports directed migration of transplanted immature neurons. *Experimental Neurology*. 1999; 157:43–57. [PubMed: 10222107]
- Lee MK, Tuttle JB, Rebhun LI, Cleveland DW, Frankfurter A. The expression and posttranslational modification of a neuron-specific beta-tubulin isotype during chick embryogenesis. *Cell Motility and the Cytoskeleton*. 1990; 17:118–132. [PubMed: 2257630]
- Leenen PJ, de Bruijn MF, Voerman JS, Campbell PA, van Ewijk W. Markers of mouse macrophage development detected by monoclonal antibodies. *Journal of Immunological Methods*. 1994; 174:5–19. [PubMed: 8083537]
- Lendahl U, Zimmerman LB, McKay RD. CNS stem cells express a new class of intermediate filament protein. *Cell*. 1990; 60:585–595. [PubMed: 1689217]
- Lois C, Alvarez-Buylla A. Proliferating subventricular zone cells in the adult mammalian forebrain can differentiate into neurons and glia. *Proceedings of the National Academy of Sciences*. 1993; 90:2074–2077.
- Lois C, Alvarez-Buylla A. Long-distance neuronal migration in the adult mammalian brain. *Science*. 1994; 264:1145–1148. [PubMed: 8178174]
- Lois C, Garcia-Verdugo JM, Alvarez-Buylla A. Chain migration of neuronal precursors. *Science*. 1996; 271:978–981. [PubMed: 8584933]
- Ludwin SK, Kosek JC, Eng LF. The topographical distribution of S-100 and GFA proteins in the adult rat brain: an immunohistochemical study using horseradish peroxidase-labelled antibodies. *Journal of Comparative Neurology*. 1976; 165:197–207. [PubMed: 1107363]
- Luskin MB. Restricted proliferation and migration of postnatally generated neurons derived from the forebrain subventricular zone. *Neuron*. 1993; 11:173–189. [PubMed: 8338665]
- Luskin MB. Neuroblasts of the postnatal mammalian forebrain: their phenotype and fate. *Journal of Neurobiology*. 1998; 36:221–233. [PubMed: 9712306]
- Magavi SS, Leavitt BR, Macklis JD. Induction of neurogenesis in the neocortex of adult mice. *Nature*. 2000; 405:951–955. [PubMed: 10879536]
- Magavi SS, Mitchell BD, Szentirmai O, Carter BS, Macklis JD. Adult-born and pre-existing olfactory granule neurons undergo distinct experience-dependent modifications of their olfactory responses in vivo. *Journal of Neuroscience*. 2005; 25:10729–10739. [PubMed: 16291946]
- Malatesta P, Hack MA, Hartfuss E, Kettenmann H, Klinkert W, Kirchhoff F, Götz M. Neuronal or glial progeny. Regional differences in radial glia fate. *Neuron*. 2003; 37:751–764. [PubMed: 12628166]
- Malatesta P, Hartfuss E, Götz M. Isolation of radial glial cells by fluorescent-activated cell sorting reveals a neuronal lineage. *Development*. 2000; 127:5253–5263. [PubMed: 11076748]
- Markakis EA, Palmer TD, Randolph-Moore L, Rakic P, Gage FH. Novel neuronal phenotypes from neural progenitor cells. *Journal of Neuroscience*. 2004; 24:2886–2897. [PubMed: 15044527]
- Marusich MF, Fumeaux HM, Henion PD, Weston JA. Hu neuronal proteins are expressed in proliferating neurogenic cells. *Journal of Neurobiology*. 1994; 25:143–155. [PubMed: 7517436]
- McMorris FA, Kim SU, Sprinkle TJ. Intracellular localization of 2',3'-cyclic nucleotide 3'-phosphohydrolase in rat oligodendrocytes and C6 glioma cells and effect of cell maturation and enzyme induction on localization. *Brain Research*. 1984; 292:123–131. [PubMed: 6320968]
- Memberg SP, Hall AK. Dividing neuron precursors express neuron-specific tubulin. *Journal of Neurobiology*. 1995; 27:26–43. [PubMed: 7643073]
- Menezes JR, Luskin MB. Expression of neuron-specific tubulin defines a novel population in the proliferative layers of the developing telencephalon. *Journal of Neuroscience*. 1994; 14:5399–5416. [PubMed: 8083744]

- Menezes JR, Smith CM, Nelson KC, Luskin MB. The division of neuronal progenitor cells during migration in the neonatal mammalian forebrain. *Molecular and Cellular Neuroscience*. 1995; 6:496–508. [PubMed: 8742267]
- Merkle FT, Mirzadeh Z, Alvarez-Buylla A. Mosaic organization of neural stem cells in the adult brain. *Science*. 2007; 317:381–384. [PubMed: 17615304]
- Murase S, Cho C, White JM, Horwitz AF. ADAM2 promotes migration of neuroblasts in the rostral migratory stream to the olfactory bulb. *European Journal of Neuroscience*. 2008; 27:1585–1595. [PubMed: 18380661]
- Nadarajah B, Parnavelas JG. Modes of neuronal migration in the developing cerebral cortex. *Nature Reviews Neuroscience*. 2002; 3:423–432.
- Nguyen-Ba-Charvet KT, Picard-Riera N, Tessier-Lavigne M, Baron-Van Evercooren A, Sotelo C, Chedotal A. Multiple roles for slits in the control of cell migration in the rostral migratory stream. *Journal of Neuroscience*. 2004; 24:1497–1506. [PubMed: 14960623]
- Noctor SC, Flint AC, Weissman TA, Dammerman RS, Kriegstein AR. Neurons derived from radial glial cells establish radial units in neocortex. *Nature*. 2001; 409:714–720. [PubMed: 11217860]
- Noctor SC, Flint AC, Weissman TA, Wong WS, Clinton BK, Kriegstein AR. Dividing precursor cells of the embryonic cortical ventricular zone have morphological and molecular characteristics of radial glia. *Journal of Neuroscience*. 2002; 22:3161–3173. [PubMed: 11943818]
- Nolte C, Matyash M, Pivneva T, Schipke CG, Ohlemeyer C, Hanisch UK, Kirchhoff F, Kettenmann H. GFAP promoter-controlled EGFP-expressing transgenic mice: a tool to visualize astrocytes and astrogliosis in living brain tissue. *Glia*. 2001; 33:72–86. [PubMed: 11169793]
- Quimet CC, Greengard P. Distribution of DARPP-32 in the basal ganglia, an electron microscopic study. *Journal of Neurocytology*. 1990; 19:39–52. [PubMed: 2191086]
- Parnavelas JG, Nadarajah B. Radial glial cells. are they really glia? *Neuron*. 2001; 31:881–884. [PubMed: 11580889]
- Peretto P, Merighi A, Fasolo A, Bonfanti L. Glial tubes in the rostral migratory stream of the adult rat. *Brain Research Bulletin*. 1997; 42:9–21. [PubMed: 8978930]
- Peretto P, Giachino C, Aimar P, Fasolo A, Bonfanti L. Chain formation and glial tube assembly in the shift from neonatal to adult subventricular zone of the rodent forebrain. *Journal of Comparative Neurology*. 2005; 487:407–427. [PubMed: 15906315]
- Peters A, Palay SL, Webster HD. *The fine structure of the nervous system: neurons and their supporting cells*. Oxford UP. 1991
- Petreanu L, Alvarez-Buylla A. Maturation and death of adult-born olfactory bulb granule neurons: role of olfaction. *Journal of Neuroscience*. 2002; 22:6106–6113. [PubMed: 12122071]
- Privat A. Postnatal gliogenesis in the mammalian brain. *International Review of Cytology*. 1975; 40:281–323. [PubMed: 1097355]
- Prochiantz A, Mallat M. Astrocyte diversity. *Annals of the New York Academy of Science*. 1988; 540:52–63.
- Puche AC, Shipley MT. Radial glia development in the mouse olfactory bulb. *Journal of Comparative Neurology*. 2001; 434:1–12. [PubMed: 11329125]
- Raff MC, Abney ER, Cohen J, Lindsay R, Noble M. Two types of astrocytes in cultures of developing rat white matter: differences in morphology, surface gangliosides and growth characteristics. *Journal of Neuroscience*. 1983; 3:1289–1300. [PubMed: 6343560]
- Rakic P. Mode of cell migration to the superficial layers of fetal monkey neocortex. *Journal of Comparative Neurology*. 1972; 145:61–83. [PubMed: 4624784]
- Rakic P. Developmental and evolutionary adaptations of cortical radial glia. *Cerebral Cortex*. 2003a; 13:541–549. [PubMed: 12764027]
- Rakic P. Elusive radial glial cells: historical and evolutionary perspective. *Glia*. 2003b; 43:19–32. [PubMed: 12761862]
- Ranscht B, Clapshaw PA, Price J, Noble M, Seifert W. Development of oligodendrocytes and Schwann cells studied with a monoclonal antibody against galactocerebroside. *Proceedings of the National Academy of Sciences*. 1982; 79:2709–2713.

- Reyher CKH, Lubke J, Larsen WJ, Hendrix GM, Shipley MT, Baumgarten HG. Olfactory bulb granule cell aggregates: morphological evidence for interperikaryal electrotonic coupling via gap junctions. *Journal of Neuroscience*. 1991; 11:1485–1495. [PubMed: 1904478]
- Rice DS, Curran T. Role of the reelin signaling pathway in central nervous system development. *Annual Review of Neuroscience*. 2001; 24:1005–1039.
- Saghatelyan A, de Chevigny A, Schachner M, Lledo PM. Tenascin-R mediates activity-dependent recruitment of neuroblasts in the adult mouse forebrain. *Nature Neuroscience*. 2004; 7:347–356.
- Schmechel DE, Rakic P. A Golgi study of radial glial cells in developing monkey telencephalon: morphogenesis and transformation into astrocytes. *Anatomy and Embryology (Berlin)*. 1979; 156:115–152.
- Schmued LC, Hopkins KJ. Fluoro-Jade B: a high affinity fluorescent marker for the localization of neuronal degeneration. *Brain Research*. 2000; 874:123–130. [PubMed: 10960596]
- Scotti Campos L. Evidence for astrocyte heterogeneity: a distinct subpopulation of protoplasmic-like glial cells is detected in transgenic mice expressing Lmo1-lacZ. *Glia*. 2003; 43:195–207. [PubMed: 12898699]
- Seri B, Garcia-Verdugo JM, McEwen BS, Alvarez-Buylla A. Astrocytes give rise to new neurons in the adult mammalian hippocampus. *Journal of Neuroscience*. 2001; 21:7153–7160. [PubMed: 11549726]
- Shapiro LA, Korn MJ, Shan Z, Ribak CE. GFAP-expressing radial glia-like cell bodies are involved in a one-to-one relationship with doublecortin-immunolabeled newborn neurons in the adult dentate gyrus. *Brain Research*. 2005; 1040:81–91. [PubMed: 15804429]
- Shewan D, Calaora V, Nielsen P, Cohen J, Rougon G, Moreau H. mCD24, a glycoprotein transiently expressed by neurons, is an inhibitor of neurite outgrowth. *Journal of Neuroscience*. 1996; 16:2624–2634. [PubMed: 8786438]
- Shibata T, Yamada K, Watanabe M, Ikenaka K, Wada K, Tanaka K, Inoue Y. Glutamate transporter GLAST is expressed in the radial glia-astrocyte lineage of developing mouse spinal cord. *Journal of Neuroscience*. 1997; 17:9212–9219. [PubMed: 9364068]
- Soriano E, Alvarez-Mallart RM, Dumesnil N, Del Rio JA, Sotelo C. Cajal-Retzius cells regulate the radial glia phenotype in the adult and developing cerebellum and alter granule cell migration. *Neuron*. 1997; 18:563–577. [PubMed: 9136766]
- Stallcup WB, Beasley L. Bipotential glial precursor cells of the optic nerve express the NG2 proteoglycan. *Journal of Neuroscience*. 1987; 7:2737–2744. [PubMed: 3305800]
- Su M, Hu H, Lee Y, d’Azzo A, Messing A, Brenner M. Expression specificity of GFAP transgenes. *Neurochemical Research*. 2004; 29:2075–2093. [PubMed: 15662842]
- Sundholm-Peters NL, Yang HK, Goings GE, Walker AS, Szele FG. Radial glia-like cells at the base of the lateral ventricles in adult mice. *Journal of Neurocytology*. 2004; 33:153–164. [PubMed: 15173638]
- Thomas LB, Gates MA, Steindler DA. Young neurons from the adult subependymal zone proliferate and migrate along an astrocyte, extracellular matrix-rich pathway. *Glia*. 1996; 17:1–14. [PubMed: 8723838]
- Trommsdorff M, Gotthardt M, Hiesberger T, Shelton J, Stockinger W, Nimpf J, Hammer RE, Richardson JA, Herz J. Reeler/Disabled-like disruption of neuronal migration in knockout mice lacking the VLDL receptor and ApoE receptor 2. *Cell*. 1999; 97:689–701. [PubMed: 10380922]
- Ventura RE, Goldman JE. Dorsal radial glia generate olfactory bulb interneurons in the postnatal murine brain. *Journal of Neuroscience*. 2007; 27:4297–4302. [PubMed: 17442813]
- Voigt T. Development of glial cells in the cerebral wall of ferrets: direct tracing of their transformation from radial glia into astrocytes. *Journal of Comparative Neurology*. 1989; 289:74–88. [PubMed: 2808761]
- Wichterle H, Garcia-Verdugo JM, Alvarez-Buylla A. Direct evidence for homotypic, glia-independent neuronal migration. *Neuron*. 1997; 18:779–791. [PubMed: 9182802]
- Winner B, Cooper-Kuhn CM, Aigner R, Winkler J, Kuhn HG. Long-term survival and cell death of newly generated neurons in the adult rat olfactory bulb. *European Journal of Neuroscience*. 2002; 16:1681–1689. [PubMed: 12431220]

- Wu W, Wong K, Chen J, Jiang Z, Dupuis S, Wu JY, Rao Y. Directional guidance of neuronal migration in the olfactory system by the protein Slit. *Nature*. 1999; 400:331–336. [PubMed: 10432110]
- Wu Y, Liu Y, Levine EM, Rao MS. Hes1 but not Hes5 regulates an astrocyte versus oligodendrocyte fate choice in glial restricted precursors. *Developmental Dynamics*. 2003; 226:675–689. [PubMed: 12666205]
- Zhuo L, Sun B, Zhang CL, Fine A, Chiu SY, Messing A. Live astrocytes visualized by green fluorescent protein in transgenic mice. *Developmental Biology*. 1997; 187:36–42. [PubMed: 9224672]

RESEARCH HIGHLIGHTS

1. We have identified a novel population of adult olfactory radial glia-like cells (AORGs).
2. AORGs are radially oriented, and restricted to the granular layer of the OB.
3. AORGs exhibit phenotypical characteristics of forebrain radial glia.
4. AORGs are generated locally throughout life, and exhibit long-term survival.
5. AORGs might likely play a role in radial neuronal migration in the postnatal OB.

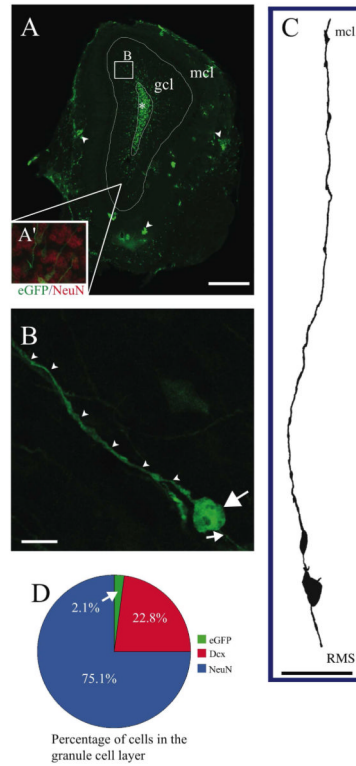


FIGURE 1. Location, morphology, and abundance of AORGs

(A) Photomontage of a coronal section of the adult OB in an hGFAP-eGFP transgenic mouse, in which eGFP is expressed under the control of a human GFAP promoter fragment, showing the position and orientation of AORGs in the granule cell layer (gcl; box B), extending their processes from the base of the RMS (asterisk) toward the gcl. Inner white line denotes outer perimeter of the RMS (*); outer white line denotes outer perimeter of the gcl; arrowheads indicate clusters of astroglia in the mitral cell layer (mcl). Inset in A (A') shows a magnified view of the granule cell layer, with NeuN in red, and AORGs in green). The box (B) in panel A denotes the approximate region from which panel B is derived. Scale bar, 500 μ m. (B) Confocal reconstruction (z-stack) of a typical AORG in the adult OB. Note the simple, elongated, and unbranched apical (arrowheads) and basal (small arrow) radial processes, and the large, round soma. Scale bar, 10 μ m. (C) *Camera lucida* drawing of a typical AORG, oriented from the RMS to the mcl. Scale bar, 50 μ m. (D) AORGs comprise a very small percentage of cells in the granule cell layer of the adult OB (2.1%), compared to mature, NeuN-positive granule cells (75.1%) and immature, Dcx-positive migrating neurons (22.8%). (AORG, adult olfactory radial glia-like cell; RMS, rostral migratory stream; gcl, granule cell layer; mcl, mitral cell layer).

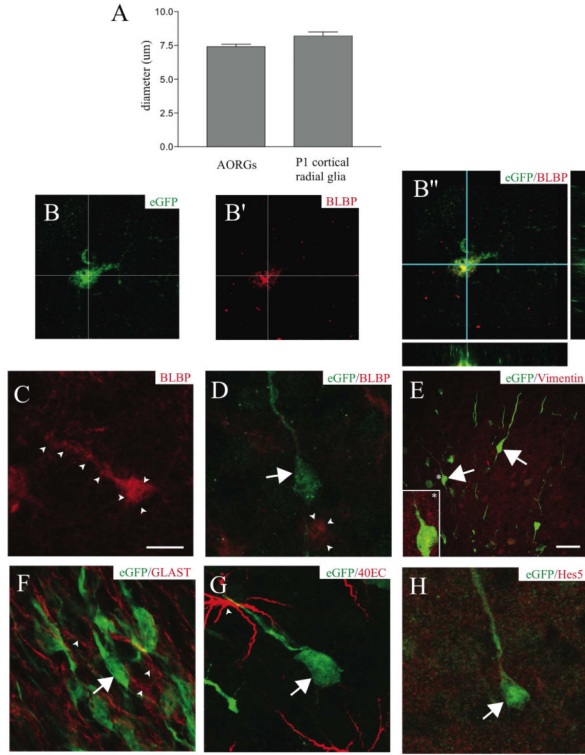


FIGURE 2. AORGs are morphologically and immunochemically similar to developmental cortical radial glia

(A) AORGs are similar in size to radial glia present during early postnatal neocortical development (6 mice per assessment). (B, B', and B'') A subset of AORGs expresses the radial glial marker BLBP, as shown with images of eGFP alone (B, green), BLBP alone (B', red) and merged (B'', shown with orthogonal reconstruction in the XZ and YZ planes). (C) Some BLBP-positive cells are eGFP-negative, but have AORG-like morphology (outlined by arrowheads). (D) Some non-radial cells express BLBP (arrowheads), and some eGFP-positive AORGs (green, arrow) do not express BLBP (red). (E-H) AORGs (green) do not express any of a panel of other radial glial markers at high level, including vimentin (E, inset, indicated by an asterisk); GLAST (F, red, arrowheads); 40EC (G, arrowhead), or Hes5 (H, red). Scale bar in (C), 10 µm for panels (B) through (D) and (F) through (H); scale bar in (E), 25 µm.

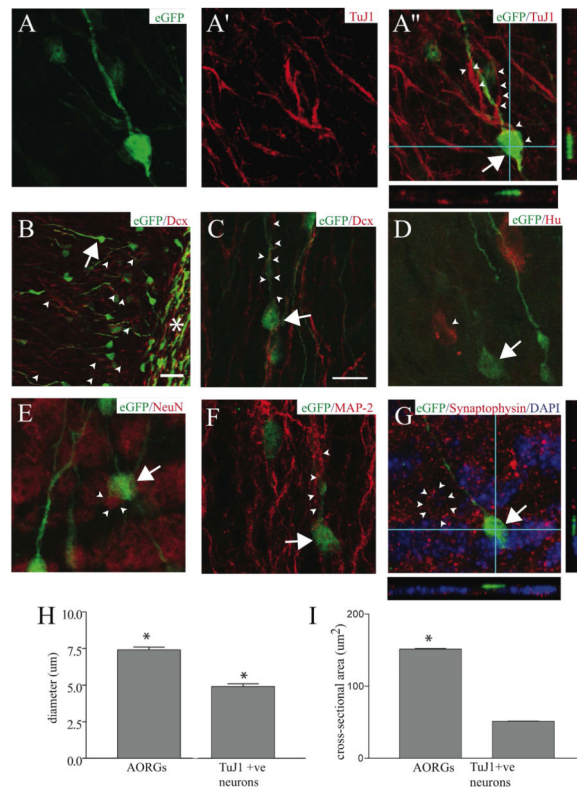


FIGURE 3. AORGs are not neurons

High magnification three-dimensional confocal reconstructions of AORGs in the adult OB indicate that AORGs (arrows; green in all panels) do not express any of a variety of markers of progressive neuronal differentiation. (A through A'') Confocal reconstruction showing an AORG in the OB (A, green) closely apposed to cells that express the immature neuronal marker TuJ1 (A', red, and merged A''); the arrow indicates the soma of the AORG, and arrowheads indicate TuJ1-positive fibers and their close apposition to the radially extended process of the AORG. AORGs do not express TuJ1. (B-G) AORGs also do not express a broad set of other immature and mature neuronal markers (shown in red). AORGs do not express the immature neuronal marker doublecortin, Dcx (B and C, arrowheads). (B) Low magnification view of the end of the RMS (asterisk), indicating substantial co-expression of eGFP and Dcx in many migrating immature neurons within and proximal to the RMS. Within the granule cell layer, there are numerous Dcx-positive cell bodies (arrowheads) and fine processes, as well as an eGFP-positive AORG (arrow). (C) High magnification image of an AORG (arrow) in close association with Dcx-positive processes of immature migrating neurons (arrowheads). (D-F) AORGs do not express the post-mitotic neuronal marker Hu (D, arrowhead), the mature neuronal nuclear marker NeuN (E, arrowheads), or the neuron-specific, somato-dendritic microtubule-associated protein MAP-2 (F, arrowheads). (G) AORGs are also not labeled by the presynaptic protein synaptophysin (neuron rimmed by synapses, arrowheads; DAPI nuclear counterstain is in blue). Panels (A'') and (G) include orthogonal reconstructions in the XZ and YZ planes to demonstrate lack of co-localization of eGFP with TuJ1 or synaptophysin. Scale bar in (C) for all panels, 10 μ m, except for (B), in which the scale bar is 25 μ m. (H, I) AORGs are significantly larger than TuJ1-positive immature neurons, in both soma diameter and cross-sectional area (*, $p < 0.0001$; 6 mice per assessment).

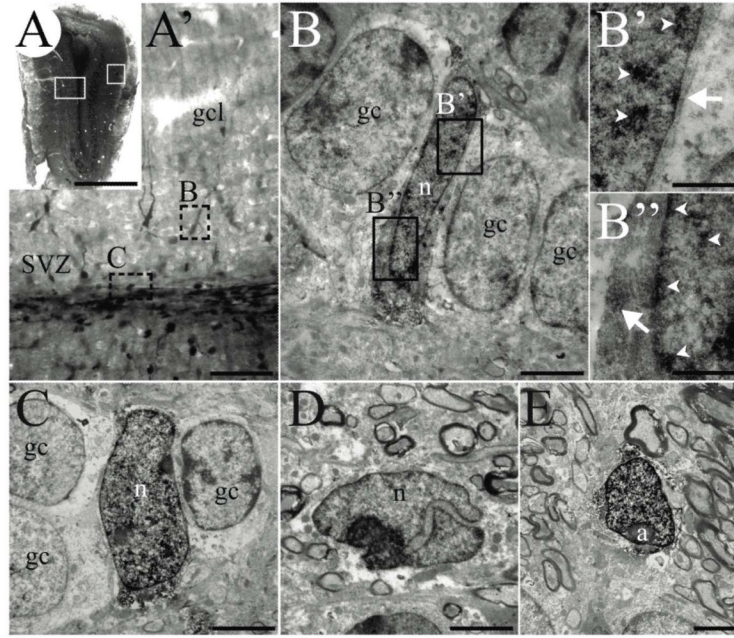


FIGURE 4. AORGs resemble immature glia ultrastructurally

(A) Photomontage of a coronal section of the adult OB from an hGFAP-eGFP transgenic mouse in which expression of GFP is reported via immunoperoxidase staining. White boxed areas (left, right) indicate approximate regions from which images shown in A' and E were obtained, respectively. (A') Higher magnification image of left boxed area in A, showing deep layers of the OB, granule cell layer, and the anterior extension of the RMS. Note that the DAB precipitate reveals cells of different intensity in the granule cell layer and SVZ. Dashed boxes indicate areas shown in B and C. (B, B', and B'') An example of an AORG, found between mature granule cells. (B' and B'') Higher magnification of boxed areas in B, showing the DAB immunoprecipitate (arrowheads indicate precipitate in nuclei; arrows indicate cytoplasmic precipitate). (C) Another example of an identified AORG positioned between granule cells. (D) An example of a neuroblast with a typical invaginated nucleus within the SVZ/RMS; such neuroblasts are usually lightly labeled. (E) A typical astrocyte in the periglomerular region. Scale bar in (A), 1 mm, (A') 250 μm ; for panels (B) through (E), 30 μm and for (B' and B''), 5 μm . (a, astrocyte; gc, granule cell; gcl, granule cell layer; n, nucleus).

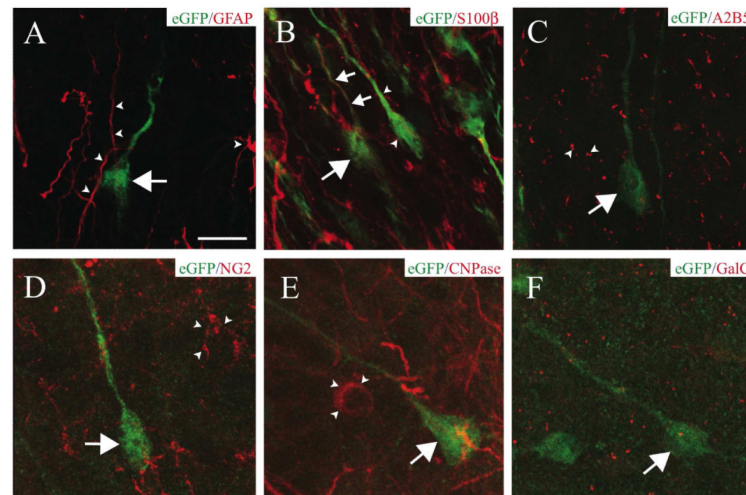


FIGURE 5. AORGs rarely express astroglial markers, and are not oligodendroglia
 (A) High magnification confocal three-dimensional reconstructions reveal that AORGs (green, arrow) do not express GFAP (red, arrowheads indicate GFAP-positive astroglial processes). (B) AORGs occasionally express S100 β ; an AORG (large arrow) with an S100 β -positive process (small arrows). AORGs are often immunonegative for S100 β (arrowheads). (C) AORGs (arrows) do not express A2B5 (arrowheads). (D-F) AORGs (arrows) do not express the oligodendroglial markers NG2 (D, arrowheads), CNPase (E, arrowheads), or GalC (F). Scale bar in (A), 10 μ m for panels A through F.

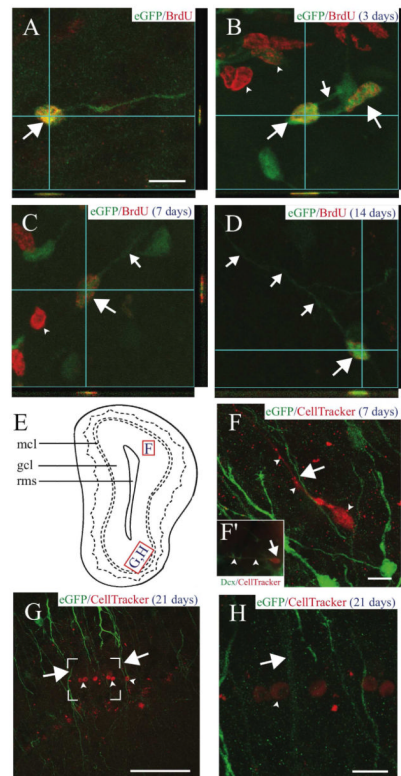


FIGURE 6. AORGs are born in the adult OB, and are closely apposed to migrating, immature neurons

(A) Newborn AORGs (arrows) are found in the adult OB granule cell layer following adult BrdU administration. Co-labeling by BrdU (red) and eGFP (green) in AORGs was confirmed by three-dimensional confocal orthogonal reconstructions in the XZ and YZ planes. (B-D) Pulse labels of BrdU demonstrate that (B) AORGs (arrows) develop short processes (small arrow) by 3 days after their birth. Note eGFP-negative/BrdU-positive cells in (B) and (C) (arrowheads, putative adult-born granule neurons). (C) AORGs extend their processes further by 7 days (small arrow), and (D) display mature AORG morphology by 14 days after their birth. (E) Schematic representation of the olfactory bulb, indicating the regions from which panels F, G, and H are derived. (F) The whole cell label CellTracker Red was injected into the adult SVZa, revealing a close association between immature, adult-born migrating neurons (red, arrowheads) and the radial process of eGFP-positive AORGs (green, arrow) 7 days after CellTracker Red injection. (F', inset) an example of a cell labeled by CellTracker Red that is immunopositive for doublecortin (Dcx, green), in the granule cell layer of the OB. Arrow indicates the cell body, and arrowheads mark the leading process of this migrating, immature neuron. (G and H) The close anatomical relationship between adult-born mature granule neurons (arrowheads) in the gcl and the radially oriented eGFP-positive fibers of AORGs (arrows) 21 days after CellTracker Red injection is shown via confocal reconstructions at lower (G; box indicates area magnified in (H)) and higher magnification (H). Scale bar in (A), 10 μ m for panels (A-D); scale bar in each of (F-H), 50 μ m. (gcl, granule cell layer; mcl, mitral cell layer; rms, rostral migratory stream). Schematic diagram based on Franklin and Paxinos (1997).

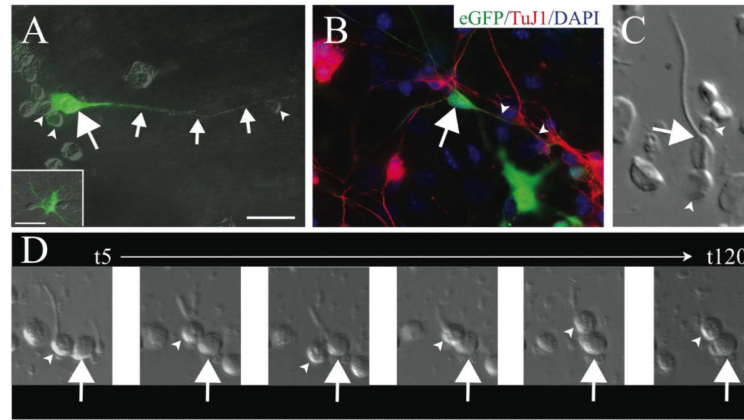


FIGURE 7. Immature OB neurons are closely apposed to AORG radial processes *in vitro* (A) Dissociated culture of the developing OB shows an eGFP-positive AORG (arrow) with an extensive linear process (small arrows). Smaller presumptive immature neurons (arrowheads) are often located in close apposition to the somas and radial processes of AORGs. In culture, as *in vivo*, AORGs are morphologically different from eGFP-positive astrocytes (inset in A). (B) Processes of TuJ1-positive immature neurons (red, arrowheads) are adjacent to the radial process of a mature AORG (arrow). (C) Dissociated cells at P14 illustrate the close apposition between immature neurons (arrowheads) and the soma and radial process of an AORG (arrow). (D) Time-lapse videomicroscopy suggests that immature neurons (arrowheads) are capable of attaching to radial processes of AORGs (arrow) and sometimes initiate migration. Representative still images are shown from t=5 minutes to t=120 minutes. Scale bar in (A) for panels (A) and (B), 25 μ m.

TABLE 1

Antibodies used for immunocytochemical characterization of AORGs

	Mono- or polyclonal	Concentration	Source
40E-C	Monoclonal	1:5	DSHB
A2B5	Monoclonal	1:250	P. Follett
ApoE	Monoclonal	1:25	Chemicon/Millipore
BLBP	polyclonal, rabbit	1:500	N. Heintz
BrdU	monoclonal, rat	1:400	Harlan
Caspase-3	polyclonal, rabbit	1:750	NEB
CD24	Monoclonal	1:100	eBioscience
CNPase	Monoclonal	1:250	Chemicon/Millipore
DAB-1	polyclonal, rabbit	1:100	Chemicon/Millipore
DARPP-32	polyclonal, rabbit	1:250	Chemicon/Millipore
Dcx	polyclonal, guinea pig	1:500	Chemicon/Millipore
F4/80	monoclonal, rat	1:100	eBioscience
GalC	polyclonal, rabbit	1:50	Chemicon/Millipore
GFAP	polyclonal, rabbit	1:500	Chemicon/Millipore
GFP	polyclonal, rabbit	1:500	Molecular Probes
GFP	polyclonal, chick	1:500	Chemicon/Millipore
GLAST	polyclonal, rabbit	1:250	Chemicon/Millipore
Glut. Synth.	polyclonal, rabbit	1:100	Sigma
Hes5	polyclonal, rabbit	1:100	Chemicon/Millipore
Hu	Monoclonal	1:100	Molecular Probes
MAP2	Monoclonal	1:500	Sigma
Nestin	Monoclonal	1:25	R. McKay
NeuN	Monoclonal	1:500	Chemicon/Millipore
NG2	polyclonal, rabbit	1:1000	Chemicon/Millipore
PSA-NCAM	Monoclonal	1:5	DSHB
RC2	Monoclonal	1:5	DSHB
Reelin	Monoclonal	1:100	Chemicon/Millipore
Slit1	polyclonal, goat	1:25	Santa Cruz
Synaptophysin	Monoclonal	1:500	Chemicon/Millipore
S100p	Monoclonal	1:250	Sigma
Tenascin-R	polyclonal, goat	1:10	Santa Cruz
Thy1.2	Monoclonal	1:100	eBioscience
TuJ1	Monoclonal	1:500	CoVance
TuJ1	polyclonal, rabbit	1:500	CoVance
Tyrosine<break/>hydroxylase	polyclonal, rabbit	1:1000	Chemicon/Millipore
Vimentin Mab<break/>3400	Monoclonal	1:100	Chemicon/Millipore
Vimentin V9	Monoclonal	1:1000	DAKO

	Mono- or polyclonal	Concentration	Source
Vimentin (ser55)	Monoclonal	1:500	Stressgen
VLDLR	polyclonal, goat	1:50	Santa Cruz